Effect of Calculation Methods on Cement Paste and Mortar Apparent Activation Energy

Article *in* Advances in Civil Engineering Materials · September 2012

DOI: 10.1520/ACEM20120011

2 authors:

Md Sarwar Siddiqui
Smislova, Kehnemui & Associates, PA
14 PUBLICATIONS **105** CITATIONS
SEE PROFILE

Kyle A. Riding
University of Florida
134 PUBLICATIONS **1,676** CITATIONS
SEE PROFILE

Advances in Civil Engineering Materials, Vol. 1, No. 1
Paper ID ACEM20120011
www.astm.org

Sarwar Siddiqui[1] *and Kyle A. Riding*[2]

Effect of Calculation Methods on Cement Paste and Mortar Apparent Activation Energy

REFERENCE: Siddiqui, Sarwar and Riding, Kyle A., "Effect of Calculation Methods on Cement Paste and Mortar Apparent Activation Energy," *Advances in Civil Engineering Materials*, Vol. 1, No. 1, 2012, pp. 1–19, doi:10.1520/ACEM20120011. ISSN 2165-3984.

ABSTRACT: Concrete hydration and strength development rates are a function of the concrete temperature, with higher temperatures leading to faster rates of reaction. The equivalent age maturity method is a commonly used method to model concrete property development under varying temperature curing conditions. The equivalent age maturity method requires the use of an activation energy value to account for the temperature sensitivity of the chemical reactions. Several experimental methods and calculation techniques are currently used to quantify the activation energy for concrete. This study compared the activation energy calculated using several different numerical methods from mortar strength, time of set, chemical shrinkage, and isothermal calorimetry paste and mortar experiments. The activation energy calculated from isothermal calorimetry experiments was found to be similar for paste and mortar. This indicates that aggregates have very little effect on the activation energy, which would permit the use of an activation energy calculated from cement paste to be used on concrete.

KEYWORDS: cement hydration, heat of hydration, chemical shrinkage, apparent activation energy, cement paste, mortar

Introduction

Many chemical reaction rates can show sensitivity to the reaction temperature. An explanation of the physical process responsible for this temperature dependence was first proposed by Swedish scientist Svante Arrhenius in 1889. The activation energy is the minimum energy required for a reaction to occur for a single reaction [1]. The higher the reaction temperature, the higher the number of molecules there will be with a kinetic energy high enough for the reaction to occur. In cement hydration, however, multiple reactions take place simultaneously, all of which are affected by temperature. The term apparent activation energy (E_a) is used to represent the average effect of temperature on the combined reactions [2]. The apparent activation energy is commonly used for strength prediction for formwork removal or load application according to the maturity method as specified in ASTM C1074 [3], cement degree of hydration (DOH), or creep calculations [4]. The accuracy of the concrete strength predicted under realistic temperatures depends on the accuracy of E_a.

Researchers have developed various methods and calculation techniques to determine the apparent activation energy of cementitious materials [3,5–11]. These methods are based on different physical property measurements of cementitious materials that develop with the progress of hydration. The strength development [3], heat of hydration [5,6], and time of set [7,8] have been used to

Manuscript received November 7, 2011; accepted for publication July 5, 2012; published online September 2012.

[1]Ph. D. Candidate, Construction Materials Research Group, The University of Texas at Austin, Austin, Texas 78758.

[2]Assistant Professor, Civil Engineering, Kansas State University, Manhattan, KS 66506-5000.

determine the activation energy for concrete. The wide variety of measurement and calculation methods can result in different E_a values, warranting further study. For example, in ASTM C1074, three calculation methods are given with no advice regarding their use.

This study is an effort to present the variability of the apparent activation energy of cementitious materials for different experimental methods and calculation techniques. Both cement mortar and paste were studied, as activation energies are often quantified using paste samples and then used to predict the properties of concrete. Although it is widely assumed that the aggregates will not affect the activation energy, no studies have been performed to confirm this assumption. The E_a was calculated from mortar cube strengths [3], time of set using the vicat apparatus [8,12] and penetration resistance [13], isothermal heat of hydration, and chemical shrinkage for a wide variety of cementitious systems in this study. The calculation techniques described in ASTM C1074 [3] (using a hyperbolic function, linear fit, and two steps method), a three parameter exponential model [10,14,15], and single linear approximation methods [9] were used to calculate the kinetic rate constant used in the Arrhenius plot to calculate the apparent activation energy. A comparison of E_a values from the different measurement and calculation techniques was made. Finally, the effect of aggregates on E_a was evaluated by comparing the values obtained from cement paste and mortar at the same water-cementitious material ratio (w/cm).

Materials

A Type I cement was used in all mixtures studied. Two fly ashes—one ASTM C618 [16] Class C and one Class F, one silica fume, one ASTM C989 [17] ground-granulated blast-furnace slag (GGBFS), and metakaolin from two different sources were used in this study. Table 1 shows the chemical composition of the materials used in this study. Table 2 shows the potential cement phases calculated by Rietveld refinement of X-ray diffraction measurements and the Bogue equations [18,19]. A sand-cementitious material ratio of 2.75 by weight was used for the mortar experiments. Table 3 shows the material proportions used. Ten mixtures of cement paste for isothermal calorimetry were also prepared with the same cementitious materials and w/cm used in the mortar experiments to compare the E_a values obtained from cement paste and mortar in isothermal calorimetry. Chemical shrinkage and time of set experiments at the higher w/cm with paste were not

TABLE 1—*Physical and chemical properties of cementitious materials.*

Properties	Type I Cement	Class C Fly Ash	Class F Fly Ash	Metakaolin 1	Metakaolin 2	Slag	Silica Fume
Specific gravity	3.2	2.8	2.4	2.2	2.7	2.5	–
SiO_2, %	21.3	31.9	55.6	50.7	52.0	33.8	90.4
Al_2O_3, %	4.7	17.8	24.0	43.6	44.4	11.5	0.14
Fe_2O_3, %	3.3	5.5	4.2	0.5	0.7	0.5	0.87
Si + Al + Fe, %	29.4	55.3	83.7	94.8	97.1	45.8	91.41
CaO, %	62.9	28.0	8.1	0.1	0.2	38.5	0.64
MgO, %	1.7	7.7	2.1	0.1	0.1	11.6	2.53
SO_3, %	2.7	2.9	0.5	0.1	0.1	2.6	0
Na_2O, %	0.1	2.2	0.7	0.3	0.3	0.3	0.15
K_2O, %	0.5	0.3	1.1	0.2	0.2	0.4	0.82
Total alkalis as Na_2O	0.5	2.4	1.4	0.4	0.4	0.5	0.69
Blaine fineness (m^2/kg)	360.1	–	–	–	–	–	–

TABLE 2—*Composition of Type I Portland cement.*

Properties	Bogue	Rietveld
C_3S (%)	49.9	67.0
C_2S (%)	23.6	16.5
C_3A (%)	7	2.9
C_4AF (%)	10	9.3
Gypsum (%)	4.6	2.3
Hemihydrate (%)	–	1.7
Arcanite (%)	–	0.2

attempted because of excessive bleeding at the higher w/cm. The fine aggregate used in this study met ASTM C33 [20] requirements.

Experimental Methods

Mixing Procedure

All mixtures were mixed at room temperature. Cement and other supplementary cementing materials (SCM) were preblended for one minute before mixing. For the mixtures used in the chemical shrinkage and isothermal calorimetry experiments for both cement paste and mortar mixtures, a small vertical laboratory mixer was used. In this procedure, water was added to the dry materials and allowed to rest for 15 s so that the cementitious material could absorb the water. The cementitious materials and water was mixed at 500 rpm for 2 min for both cement paste and mortar. For mortar samples, the fine aggregates were slowly added to the mix over the first 2 min. The mix was

TABLE 3—*Cement paste material proportions.*

Type	Mixes	Description
Cement paste	Ty I	100 % Type I cement; w/cm = 0.35
	25 % C	75 % Type I cement + 25 % Class C fly ash; w/cm = 0.35
	25 % F	75 % Type I cement + 25 % Class F fly ash; w/cm = 0.35
	15 % M-1	85 % Type I cement + 15 % metakaolin-1; w/cm = 0.35
	15 % M-2	85 % Type I cement + 15 % metakaolin-2; w/cm = 0.35
	6 % SF	94 % Type I cement + 6 % silica fume; w/cm = 0.35
	25 % S	75 % Type I cement + 25 % slag; w/cm = 0.35
	WRA	100 % Type I cement with water reducing admixture; w/cm = 0.35
	5 % C, 20 % F	75 % Type I cement + 5 % Class C + 20 % Class F fly ash; w/cm = 0.35
	20 % C, 5 % F	75 % Type I cement + 20 % Class C + 5 % Class F fly ash; w/cm = 0.35
Mortar/cement	TyI-0.5	100 % Type I cement; w/cm = 0.5
Paste mixtures to match mortar in isothermal calorimetry	TyI-0.45	100 % Type I cement; w/cm = 0.45
	25 % C	75 % Type I cement + 25 % Class C fly ash; w/cm = 0.45
	25 % F	75 % Type I cement + 25 % Class F fly ash; w/cm = 0.45
	10 % M-1	90 % Type I cement + 10 % metakaolin-1; w/cm = 0.45
	5 % SF	95 % Type I cement + 5 % silica fume; w/cm = 0.45
	25 % S	75 % Type I cement + 25 % slag; w/cm = 0.45
	WRA	100 % Type I cement with water reducing admixture; w/cm = 0.4
	5 % C, 20 % F	75 % Type I cement + 5 % Class C + 20 % Class F fly ash; w/cm = 0.45
	20 % C, 5 % F	75 % Type I cement + 20 % Class C + 5 % Class F fly ash; w/cm = 0.45

then allowed to rest for another 2 min followed by mixing for another 3 min at 2000 rpm. Mixing was performed according to ASTM C305 [21] for the larger paste and mortar samples required for mortar strength and time of set testing.

Mortar Strength

ASTM C1074 [3] specifies the use of mortar cube compressive strength tests for the determination of E_a for concrete maturity calculations. Mortar cubes were prepared and strengths were measured following ASTM C109 [22]. Three 50 mm × 50 mm (2 in. × 2 in.) mortar cubes were made and tested for compressive strength for each of the six different ages tested. The cubes were cured in saturated lime water at three different temperatures: 5°C (41°F), 23°C (73°F), and 60°C (140°F). For cubes cured at 5°C (41°F), strength tests were performed at 1, 2, 4, 8, 16, and 32 days. For cubes cured at 23°C (73°F), strength tests were performed at 12 h, 1, 2, 4, 8, and 16 days. Finally, for cubes cured at 60°C (140°F), strength tests were performed at 6 h, 12 h, 1, 2, 4, and 8 days to capture the faster rate of reaction.

Time of Set

The concept of using the setting time as a measure of degree of hydration was first proposed by Pinto and Hover [7], inspired from earlier research by Freiesleben-Hansen and Pedersen [23]. There are different ways of determining time of set for cementitious material [12,13,24]. In this study, vicat needle testing according to ASTM C191 [12] was used for cement pastes, whereas the penetration resistance according to ASTM C403 [13] was used for mortars to measure the time of set. Although the vicat needle testing was not done with a cement paste of normal consistency, the vicat needle test method has been used before on cementitious materials of various w/cm [25]. The cement paste and mortar setting time was measured at three different curing temperatures: 5°C (41°F), 23°C (73°F), and 60°C (140°F).

Heat of Hydration

Cementitious materials gain strength from the exothermic reaction between cement and water. This generated heat can be used as a measurement of the cementitious system degree of hydration [26]. In this study, the heat of hydration was measured using an eight-channel isothermal calorimeter at five different temperatures: 5°C (41°F), 15°C (59°F), 23°C (73°F), 38°C (100°F), and 60°C (140°F). The total heat of hydration was calculated by integrating the heat of hydration rate with time.

Chemical Shrinkage

Chemical shrinkage can be a measure of the cement degree of hydration and therefore, can be used to calculate E_a. Chemical shrinkage can be quantified by measuring the change in volume (first developed by Geiker [27] and then adopted as ASTM C1608 [28]) or by the change in buoyancy in a cement paste [27,29,30]. In this study, the volumetric chemical measurement technique was used.

Plastic vials were used as the sample containers. The cement paste or mortar sample was placed in the bottom of the sample container, with distilled water carefully placed above the sample to avoid mixing. A rubber stopper with a glass pipette inserted through a hole in center of the stopper was then placed in the top of the vial. After the rubber stopper was inserted at the top of the sample container, the pipette was filled with water followed by a small amount of colored petrol with a lower density than water. A temperature controlled water bath was used to maintain a constant curing

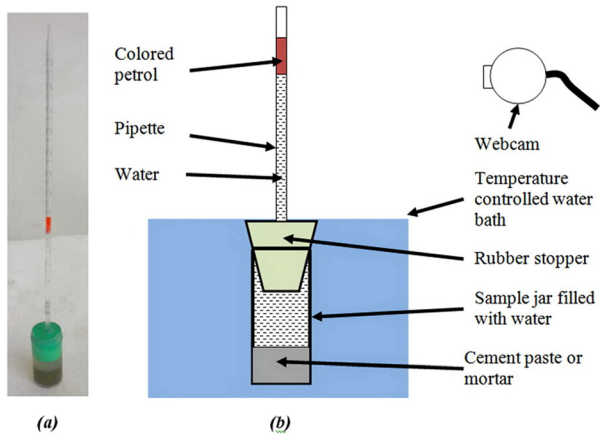

FIG. 1—*Chemical shrinkage (a) sample, and (b) schematic diagram of chemical shrinkage bath.*

temperature. A webcam was used to take pictures of the water level in the pipette by monitoring the bottom of the colored petrol level. Figure 1 shows the sample and schematic diagram of the chemical shrinkage setup. Automatic image analysis of the pipette water level was performed using the LMC Shrinkage Suite software developed by S. Bishnoi in 2008. The chemical shrinkage for each mixture was taken as the average of four samples. Chemical shrinkage was measured for both cement paste and mortar at three different temperatures: 5°C (41°F), 23°C (73°F), and 38°C (100°F).

Calculation Techniques

Several different calculation methods were used to obtain the rate constant value k in the Arrhenius equation shown in Eq 1.

$$k = Ae^{-\frac{E_a}{RT}} \tag{1}$$

where R = universal gas constant (8.314 J/mol/K), T = temperature (K) at which the reaction occurs, k = the rate of heat evolution (W), A = the proportionality constant (same units as k), and E_a = apparent activation energy (J/mol). E_a was then calculated as the universal gas constant R (=8.314 Jmole^{-1}k^{-1}) multiplied by the slope of a line fit to the ln(k) versus 1/T values. The plot of ln(k) versus 1/T is known as the Arrhenius plot. Not all of the calculation methods were applicable to all of the experimental methods. Table 4 contains a summary of the experimental and calculation methods used for calculating E_a in this study.

The single linear approximation method is the simplest method for calculating E_a from isothermal calorimetry or chemical shrinkage data [9]. The slope of the linear part of the acceleration phase of the cement hydration was used for this method as the rate constant k [9].

ASTM C1074 specifies three methods for determination of E_a from mortar cube strength [3]. These techniques vary only by the calculation method used to obtain the rate constant k. For the linear fit method, the k-value for different temperatures was determined by plotting the reciprocal of age of the strength test after the final set as the abscissa and reciprocal of strength as the ordinate. This technique was only used for the mortar cube strength method.

The hyperbolic function method outlined in ASTM C1074 uses a hyperbolic equation to fit the property development with time as shown in Eq 2:

TABLE 4—*Summary of experimental and calculation methods used.*

	Experimental Method	Single Linear Approximation	Linear Fit	Hyperbolic-E	Hyperbolic-U	Two Steps	Exponential-E	Exponential-U	Initial Time of Set	Final Time of Set
Paste	Time of set: vicat apparatus								x	x
	Isothermal calorimetry	x		x	x		x			
	Chemical shrinkage			x	x		x	x		
Mortar	Compressive strength		x		x	x				
	Time of set: penetration resistance								x	x
	Chemical shrinkage			x	x		x	x		
	Isothermal calorimetry	x		x	x		x			

$$S = S_u \frac{k(t - t_o)}{1 + k(t - t_o)} \tag{2}$$

where S = cumulative heat of hydration/chemical shrinkage/average cube compressive strengthen at the age t, S_u = ultimate cumulative heat of hydration/ultimate chemical shrinkage/limiting strength, t_o = age when heat of hydration/chemical shrinkage/strength development is assumed to begin, and k = the rate constant. In the conventional method outlined in ASTM C1074, S_u, t_o, k were determined by regression analysis for each temperature individually. This method will be referred to as the hyperbolic-U method. For determination of the E_a from the total heat of hydration and chemical shrinkage, the S_u, t_o, and k at 23°C (73°F) were first determined. t_o and k for the other curing temperatures were then determined while the S_u value was kept equal to the value determined at 23°C (73°F). This technique will be referred to as hyperbolic-E in this paper.

The last method outlined in ASTM C1074 for calculating E_a is called the two steps method in this study. This method determines the k-value from mortar strength values in two steps. First, a plot of the reciprocal of strength (ordinate) versus the reciprocal of age (abscissa) was made using the strength values from the last four sample ages. The reciprocal of the y axis intercept value is the limiting strength S_u. The values of A using the first four test ages were then calculated according to Eq 3 for each temperature:

$$A = \frac{S}{(S_u - S)} \tag{3}$$

A plot of A versus age was then made for each curing temperature, where the slope of a best-fit straight line for each curing temperatures was the k-value for that temperature. This method was used for mortar compressive strength only. E_a was then calculated from the Arrhenius plot discussed earlier.

To calculate E_a from isothermal calorimetry and chemical shrinkage, a three-parameter exponential hydration function shown in Eq 4 was used as described in previous studies [10,14,15]. The three-parameter exponential function shown in Eq 4 was considered to be a better representation of property development than the previous methods because the property values before setting are non-zero [10]:

$$H(t_e) = H_{\text{ult}} \cdot e^{-\left[\frac{\tau}{t_e}\right]^{\beta}} \tag{4}$$

where $H(t_e)$ = total heat evolved/total chemical shrinkage at equivalent time t_e, H_{ult} = total ultimate heat/chemical shrinkage, τ = the hydration time parameter (h), and β = the hydration shape parameter. In this study H_{ult}, τ, and β were first determined for the 23°C temperature data through a least squares fit. The H_{ult} and β values for the cementitious system at the other temperatures were set equal to the value found at 23°C. This uses the assumption that the shape of those property development curves remains the same for the materials at different temperatures for the studied time period. The τ for a temperature was then fitted to the experimental data at that temperature using a least squares fit. The different τ values for each of the temperatures were then used as the rate constants in the Arrhenius plot. For chemical shrinkage tests, E_a was also calculated by fitting H_{ult}, β, and τ individually for each temperature, with the τ values still used as the rate constants. This was done as the ultimate chemical shrinkage may be dependent on the curing temperature. The first method used for heat of hydration and chemical shrinkage will be referred to as exponential-E and the later one for chemical shrinkage as exponential-U.

It has been shown that the E_a of cementitious materials can be calculated from the initial or final setting time at different temperatures [7]. The inverse of the setting time is used as the rate constant k in this method.

Results and Discussion

Calculated E_a values were compared for cement paste and mortar samples to investigate the variability in E_a. The time of set, compressive strength results, and calculated activation energies are shown in Tables 5–7. Sample curve fitting of exponential-E and hyperbolic-E are shown in Fig. 2(*a*) and 2(*b*) respectively for isothermal calorimetry. More experimental values for all of the cement and mortar mixtures are found elsewhere [31].

Apparent activation energy from setting time and total heat of hydration for both cement paste and mortar are presented in Fig. 3(*a*) and 3(*b*). For both the cement paste and mortar, E_a values calculated from setting time (both initial and final setting time) measurements give much lower values than those from the isothermal total heat of hydration for the two calculation techniques. This can be explained by the fact that E_a is an empirical fit of the composite system of multiple reactions progressing during hydration. Before set, the reactions of the silicate and aluminate phase reactions and interactions will be different than after setting, which is evidenced by the difference in the time of the peak hydration rate for alite and aluminate when the sulfate content is changed. The E_a values for the time of set experiments were found to be lower than values documented in earlier studies [7,8]. Pinto and Hover [7] mixed their specimens at room temperature, and found much higher activation energies, whereas the activation energies calculated by Garcia et al. [8] were much closer to those measured in this study. Both studies used the internal temperature of the

TABLE 5—*Time of set (in minutes) at different curing temperature.*

	Curing Temperature	5°C		23°C		60°C	
	Mixes	Initial Set	Final Set	Initial Set	Final Set	Initial Set	Final Set
Cement paste	Ty I	575	769	277	417	100	147
	25 % C	657	1076	329	502	123	168
	25 % F	694	1008	340	517	132	177
	15 % M-1	524	815	215	326	101	129
	15 % M-2	485	844	221	337	95	162
	6 % SF	557	1045	240	361	95	138
	25 % S	689	1052	249	377	109	146
	WRA	884	1345	547	671	202	256
	5 % C, 20 % F	716	1061	363	475	148	198
	20 % C, 5 % F	704	1053	340	513	141	202
Mortar	TyI-0.5	499	685	238	294	115	143
	TyI-0.45	461	608	223	279	101	123
	25 % C	680	987	296	359	139	177
	25 % F	699	1045	311	391	123	185
	10 % M-1	322	476	186	254	74	100
	5 % SF	406	566	210	288	94	129
	25 % S	462	597	220	288	97	126
	WRA	744	1127	421	506	165	254
	5 % C, 20 % F	674	966	296	371	130	169
	20 % C, 5 % F	697	997	309	371	125	185

TABLE 6—*Compressive strength of mortar.*

		Compressive Strength (Mpa)									
Temperature	Time (days)	TyI-0.5	TyI-0.45	0.5 % WRA	25 % F	25 % C	25 % S	10 % M-1	5 % SF	5 % C, 20 % F	20 % C, 5 % F
5°C	1	3.42	3.50	3.04	0.90	2.26	3.87	5.97	4.49	1.96	2.25
	2	8.08	12.40	14.33	6.87	10.00	11.63	15.85	14.04	9.05	9.91
	4	20.08	26.24	27.61	16.58	18.82	19.63	28.16	24.18	19.03	18.59
	8	32.64	35.88	39.61	23.58	30.74	28.32	36.59	31.40	25.43	27.44
	16	40.86	44.10	43.63	34.51	43.29	38.50	48.44	37.23	32.03	35.14
	32	50.31	55.60	47.05	42.06	44.67	45.65	53.26	48.46	37.94	43.41
23°C	0.5	4.63	8.70	7.42	4.88	2.46	4.78	8.58	6.18	4.88	1.94
	1	14.20	21.13	22.71	9.74	13.16	16.31	20.06	16.77	9.74	11.92
	2	23.00	28.47	35.77	19.89	24.78	25.04	26.32	29.46	19.89	20.53
	4	29.18	38.98	42.09	29.17	31.14	34.14	39.40	35.30	29.17	31.96
	8	35.58	45.99	46.94	39.54	35.77	47.76	46.33	42.04	39.54	40.82
	16	44.06	50.75	53.86	45.56	46.13	51.93	58.19	52.14	45.56	50.18
60°C	0.25	3.31	6.11	0.61	2.18	1.47	5.70	9.86	8.42	2.95	4.07
	0.5	11.99	18.51	9.79	10.66	13.89	16.85	23.61	16.03	11.82	10.83
	1	22.55	26.80	28.66	17.48	20.58	23.53	31.07	26.00	20.83	17.57
	2	30.38	35.21	37.30	28.72	34.05	39.13	35.75	35.56	31.83	32.98
	4	39.70	40.43	43.03	40.43	44.32	43.44	41.82	42.38	39.32	37.09
	8	42.72	48.80	46.38	44.82	47.87	46.18	48.86	47.79	44.21	42.71

concrete for E_a calculation, which considers the effect of temperature rise of the concrete as a result of the heat of hydration. In this study, the curing temperature was used for E_a calculation in this study, potentially accounting for the difference in calculated E_a values. E_a values calculated from the final setting time gives slightly higher values than E_a values calculated from the initial setting time, shown in Fig. 4. The relationship between initial and final setting time E_a values calculated from mortar ($R^2 = 0.5648$) shows better agreement than E_a values calculated from cement paste ($R^2 = 0.4494$).

Comparison between different calculation techniques for total heat of hydration is presented in Fig. 5(*a*)–5(*d*). The hyperbolic-E method gives slightly higher E_a values than the exponential-E method, but in a predictable manner ($R^2 = 0.9082$) as shown in Fig. 5(*a*). The hyperbolic function does not model the hydration before setting time, whereas S-curves, such as the three parameter function used, do not have that limitation. The good correlation between these two methods shows how well both equations fit the total heat of hydration and represent their temperature sensitivity. Other calculation techniques for the total heat of hydration did not show any significant relation.

For mortar strength from ASTM C1074, linear fit E_a values do not show any significant relation with the ASTM C1074 hyperbolic function E_a, shown in Fig. 6(*a*). These methods have two different approaches for finding k values. The hyperbolic function considers k from curve fitting and is more influenced by the later-age strength development. The linear fit is more oriented to the early-age behavior of strength development. The ASTM C1074 two steps method gives slightly lower values than the ASTM C1074 hyperbolic function but showed good correlation with each other ($R^2 = 0.8596$) and is shown in Fig. 6(*b*).

TABLE 7—*Summary of apparent activation energy.*

	Experimental Methods	Isothermal Calorimeter				Chemical Shrinkage				Time of Set		Mortar Strength		
	Calculation Techniques	Exponential-E	SLA	Hyperbolic-E	Hyperbolic-U	Exponential-E	Exponential-U	Hyperbolic-E	Hyperbolic-U	Initial	Final	Hyperbolic	Linear Fit	Two Parameter
Cement paste	Ty I	35 140	29 419	39 137	34 766	36 078	37 398	35 624	45 296	24 323	23 137	x	x	x
	25 % C	36 564	30 045	40 728	32 330	35 914	36 938	41 530	52 338	23 220	25 786	x	x	x
	25 % F	33 217	28 620	36 456	34 808	41 826	31 383	45 056	25 748	22 950	24 266	x	x	x
	15 % M-1	35 479	32 102	40 399	40 222	30 134	30 973	29 130	27 535	22 343	25 213	x	x	x
	15 % M-2	35 352	31 106	39 923	39 177	29 327	36 260	25 450	35 468	22 345	22 341	x	x	x
	6 % SF	33 703	28 677	37 414	35 683	27 183	33 990	33 230	39 811	24 272	27 554	x	x	x
	25 % S	38 367	29 768	42 529	30 836	29 354	33 256	28 987	43 933	24 991	26 904	x	x	x
	WRA	32 412	29 215	35 290	40 718	32 634	27 949	37 412	41 006	20 789	23 001	x	x	x
	5 % C, 20 % F	34 506	27 532	39 057	34 483	33 445	34 755	31 946	38 752	21 805	23 034	x	x	x
	20 % C, 5 % F	35 244	27 890	38 892	34 539	27 790	38 856	21 559	48 042	22 116	22 827	x	x	x
Cement paste - same proportions as mortar without fine aggregate	TyI-0.5	32 250	30 311	34 878	34 003	x	x	x	x	x	x	x	x	x
	TyI-0.45	33 532	30 450	36 287	32 510	x	x	x	x	x	x	x	x	x
	25 % C-0.45	35 612	31 613	38 927	30 203	x	x	x	x	x	x	x	x	x
	25 % F-0.45	32 203	29 574	36 674	32 137	x	x	x	x	x	x	x	x	x
	10 % M-1-0.45	34 458	31 776	38 691	36 553	x	x	x	x	x	x	x	x	x
	5 % SF-0.45	33 188	31 788	35 602	36 894	x	x	x	x	x	x	x	x	x
	25 % S-0.45	37 495	31 178	40 604	27 379	x	x	x	x	x	x	x	x	x
	WRA-0.45	30 292	28 301	33 079	34 276	x	x	x	x	x	x	x	x	x
	5 % C, 20 % F-0.45	33 509	32 211	36 298	34 223	x	x	x	x	x	x	x	x	x
	20 % C, 5 % F-0.45	35 829	33 148	38 932	32 757	x	x	x	x	x	x	x	x	x

TABLE 7. *Continued*

	Experimental Methods	Isothermal Calorimeter				Chemical Shrinkage				Time of Set		Mortar Strength		
	Calculation Techniques	Exponential-E	SLA	Hyperbolic-E	Hyperbolic-U	Exponential-E	Exponential-U	Hyperbolic-E	Hyperbolic-U	Initial	Final	Hyperbolic	Linear Fit	Two Parameter
Mortar	TyI-0.5	33 394	33 040	35 685	34 922	24 831	34 682	17 960	45 000	20 105	21 304	34 922	47 631	34 326
	TyI-0.45	36 013	32 871	39 010	33 334	21 435	33 909	17 232	43 772	20 820	21 877	33 334	45 449	33 446
	25 % C	35 882	32 528	39 116	33 133	22 561	34 318	15 345	43 060	23 901	23 399	33 133	42 006	29 344
	25 % F	33 705	31 472	36 281	35 505	22 540	31 297	16 220	40 445	21 649	23 159	35 505	45 114	27 737
	10 % M-1	35 694	31 867	40 018	36 625	25 295	32 819	21 480	31 677	20 450	21 635	36 625	46 666	36 626
	5 % SF	34 324	31 614	37 338	35 196	28 099	33 346	24 612	39 694	20 170	20 365	35 196	35 174	30 673
	25 % S	38 764	30 902	41 839	26 909	24 742	30 839	15 289	38 527	21 402	21 408	26 909	39 479	38 555
	WRA	31 744	30 882	34 938	30 604	21 484	20 906	21 559	23 425	21 058	20 252	30 604	32 092	29 274
	5 % C, 20 % F	34 378	30 865	37 499	33 630	26 518	33 952	21 959	36 093	22 531	23 650	33 630	38 521	28 617
	20 % C, 5 % F	35 841	32 052	39 084	31 993	29 183	33 972	26 472	35 274	23 616	22 709	31 993	37 236	30 190

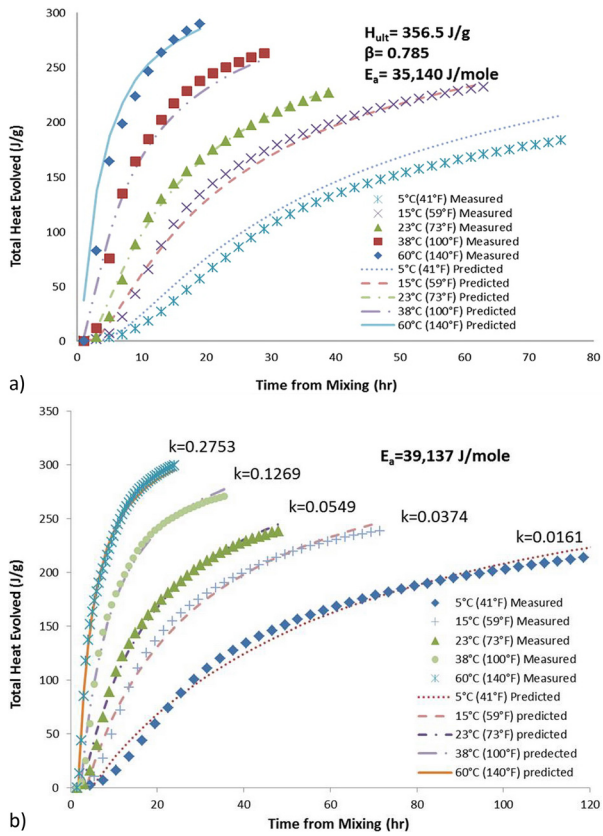

FIG. 2—*(a) Sample exponential-E fit for isothermal calorimetry, and (b) sample hyperbolic-E fit for isothermal calorimetry.*

E_a values calculated from mortar strength using the ASTM C1074 linear fit method gave relatively higher values than the value calculated using the exponential-E method from isothermal calorimetry, as shown in Fig. 7. However, E_a values from mortar strength using the ASTM C1074 hyperbolic function result in relatively lower values than the total heat of hydration for both exponential-E and hyperbolic-E. The ASTM C1074 two steps method results in lower E_a values than the exponential-E and hyperbolic-E calculated values from the total heat of hydration. The difference between the E_a values determined form isothermal calormetry and mortar cube compressive strength are probably because isothermal calorimetry measures only the rate of hydration by measuring evolved hydration heat whereas, mortar compressive strength depends on hydration rate, volume, and distribution of the porosity in matrix, and the microstructure of the hydrated product. This reinforces the idea that higher DOH does not always result in higher strength [32].

ASTM C1074 hyperbolic-E and exponential-E method E_a values, calculated from chemical shrinkage data, correlate well as shown in Fig. 8(*a*). Thus, both equations fit well with the chemical shrinkage development curve. Mortar E_a, calculated by ASTM C1074 hyperbolic-E, gives lower values, and cement paste sample ($R^2 = 0.7087$) shows better correlation than mortar samples ($R^2 = 0.5406$). E_a values calculated using the hyperbolic-U and exponential-U method do not show any significant relationship, which is shown in Fig. 8(*b*).

The potential of chemical shrinkage was evaluated by comparing the E_a values obtained from chemical shrinkage with the total heat of hydration as shown in Fig. 9. Chemical shrinkage showed

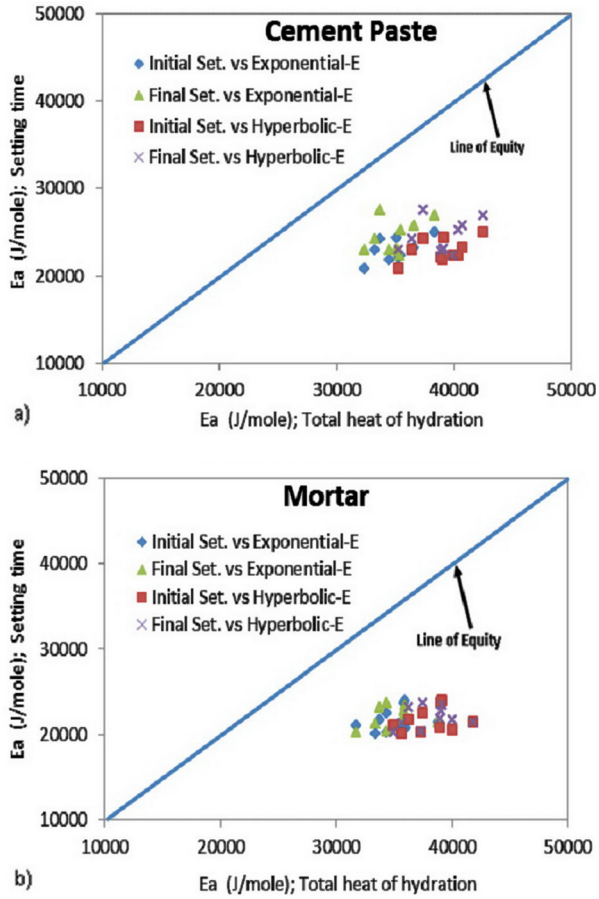

FIG. 3—*Comparison of E_a value; setting time versus total heat of hydration: (a) cement paste, and (b) mortar.*

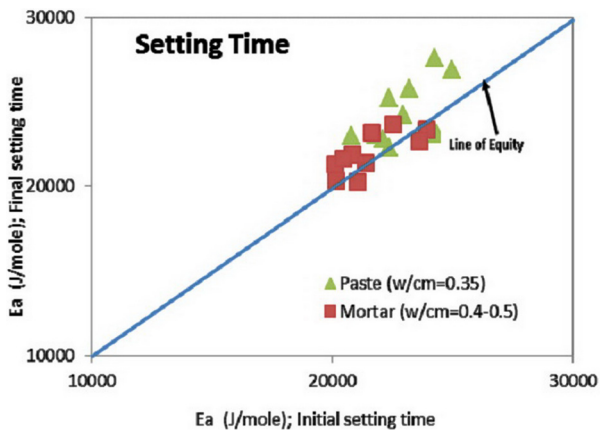

FIG. 4—*Comparison of E_a value calculated from initial and final setting time.*

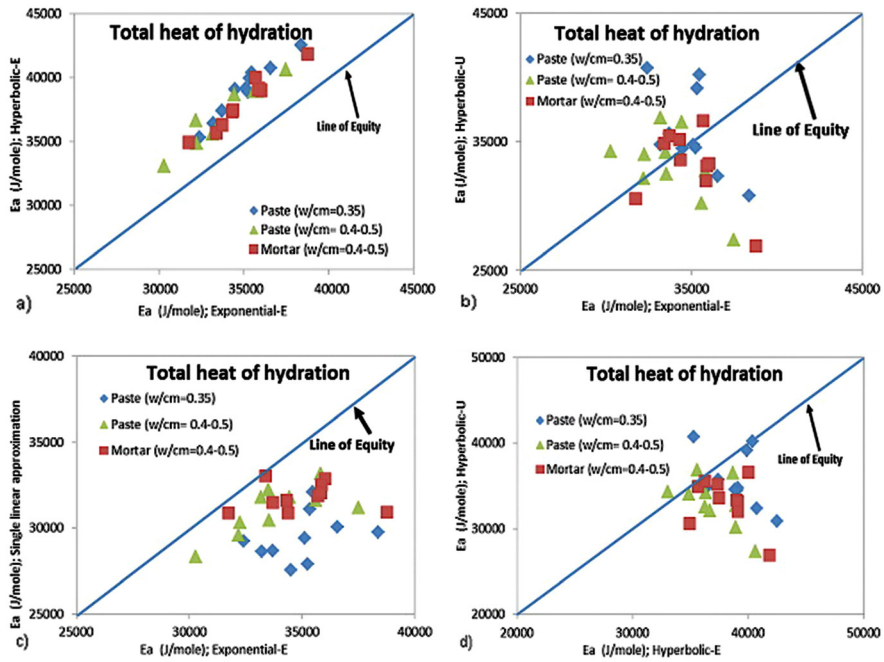

FIG. 5—*Comparison of different calculation techniques for total heat of hydration: (a) ASTM C 1074 hyperbolic-E versus exponential-E, (b) ASTM C1074 hyperbolic-U versus exponential-E, (c) single linear approximation versus exponential-E, and (d) ASTM C1074 hyperbolic-U versus ASTM C1074 hyperbolic-E.*

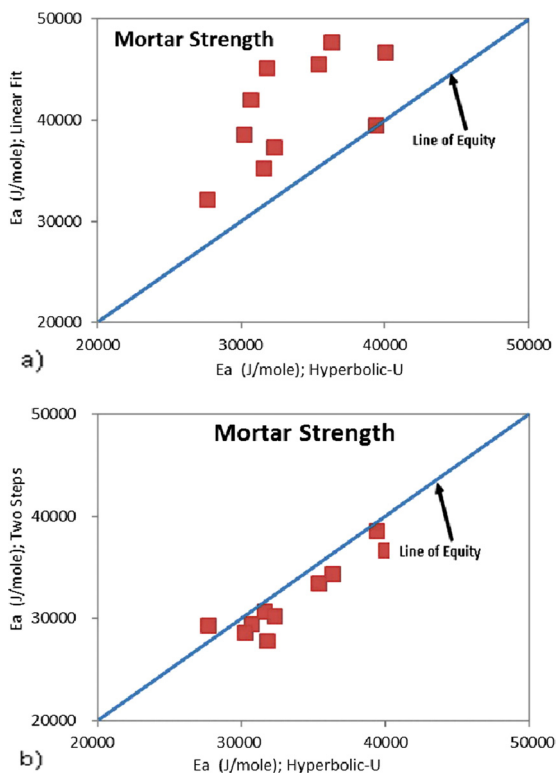

FIG. 6—*Comparison of calculation techniques for mortar strength: (a) ASTM C1074 linear fit versus ASTM C1074 hyperbolic-U, and (b) ASTM C1074 two steps method versus ASTM C1074 hyperbolic-U.*

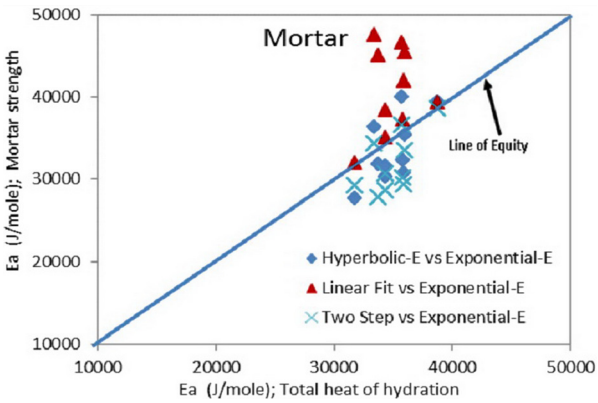

FIG. 7—*Comparison of E_a values for mortar strength versus total heat of hydration.*

lower E_a values than total heat of hydration in most case because; chemical shrinkage is lower at higher curing temperature [33]. The exponential-U method gave the best results as compared to that from isothermal calorimetry, apart from the mixtures containing a water reducing admixture. The water reducing admixture may be entraining air. These air bubbles may affect the chemical

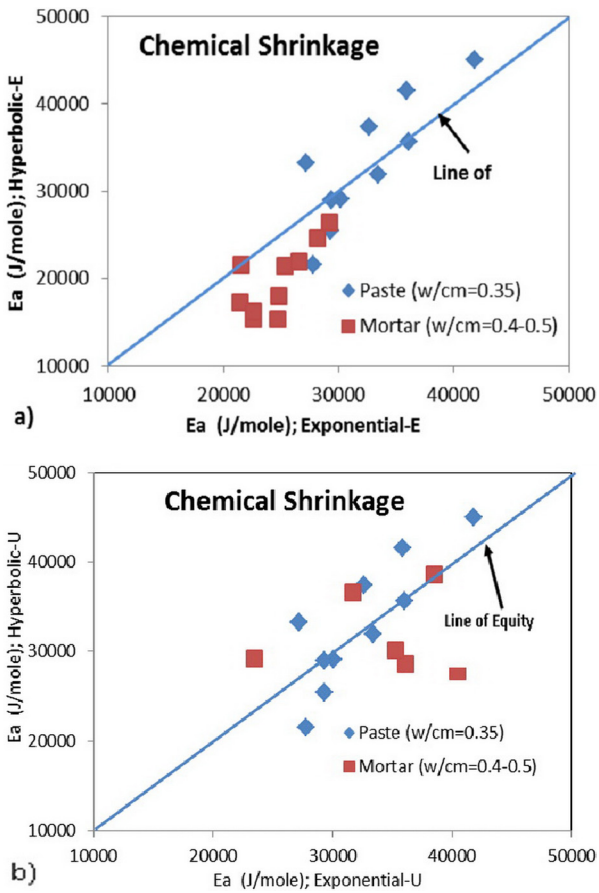

FIG. 8—*Comparison of different calculation techniques for chemical shrinkage; (a) ASTM C1074 hyperbolic-E versus exponential-E, and (b) hyperbolic-U versus exponential-U.*

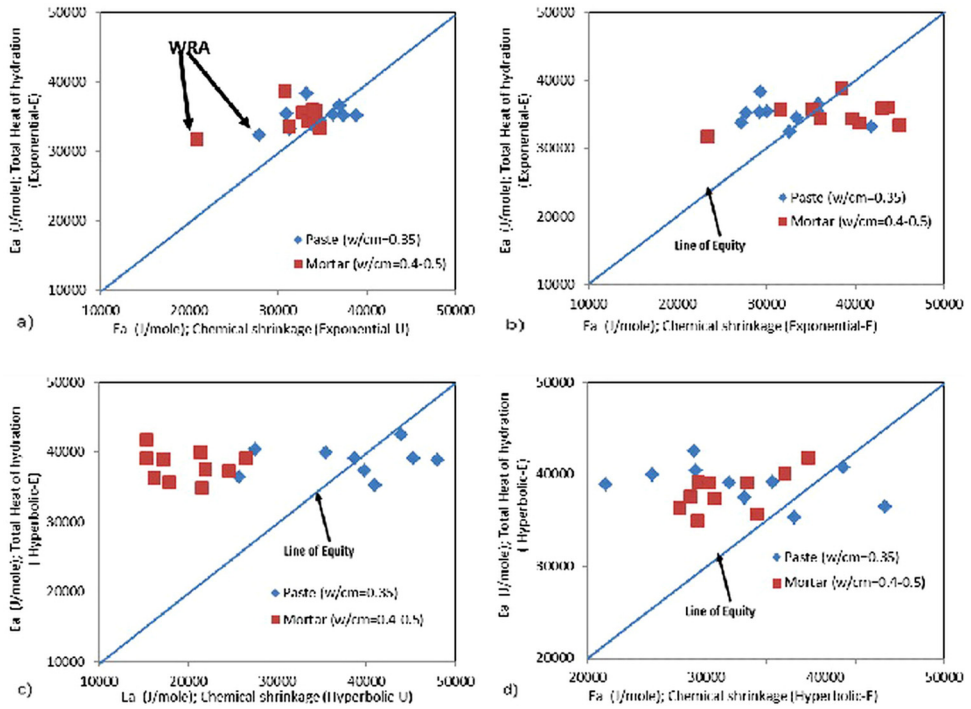

FIG. 9—*Evaluating chemical shrinkage as a mean of E_a calculation: (a) total heat of hydration, exponential-E versus chemical shrinkage, exponential-U, (b) total heat of hydration, exponential-E versus chemical shrinkage, exponential-E, (c) total heat of hydration, hyperbolic-E versus chemical shrinkage, hyperbolic-U, and (d) total heat of hydration, hyperbolic-E versus chemical shrinkage, hyperbolic-E.*

shrinkage giving erroneous results. Other studies have shown that the amount of chemically bound water for a given degree of hydration is dependent on the temperature and might explain why the exponential-U method gave the best results when compared to the isothermal calorimetry [34].

Mortar versus Cement Paste

Both cement paste and mortar results show very similar E_a values for three different calculation techniques from the cumulative heat of hydration as shown in Fig. 10. This means that there was no significant effect of aggregates on the apparent activation energy of cementitious materials for

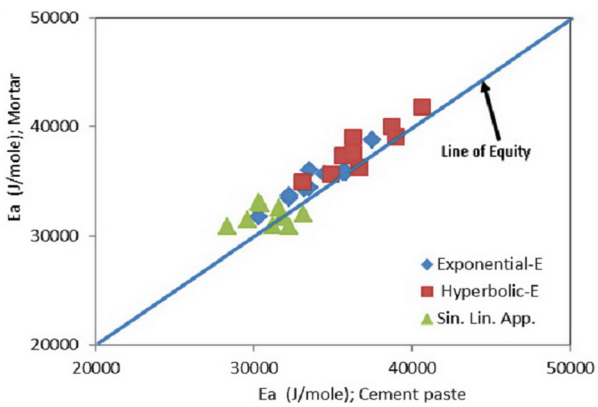

FIG. 10—*Comparison of mortar versus cement paste E_a values calculated from isothermal calorimetry.*

all of the calculation methods used. Any small effects of the aggregates on the cement hydration did not affect the temperature sensitivity for the mixtures studied. For example, the mixtures with WRA showed more retardation in the cement paste at all temperatures studied than the mortar mixtures. The activation energies were similar (less than 5 % difference) however an increase in temperature increased the hydration rate by a similar proportionate amount for each mixture.

There has been some concern that mixtures that show abnormally extended setting times or suffer from cement and admixture interaction problems could have very different hydration developments depending on whether or not aggregates are used and the mixing conditions. High amounts of agitation during mixing such as the type used in this study for isothermal calorimetry may slightly affect the hydration and the activation energy for these sensitive mixtures. These mixtures are not desirable from a quality control/constructability point of view, and were beyond the scope of this study.

Conclusions

From the experimental and calculated results, the following conclusion can be drawn:

- There is a significant effect of calculation methods on the E_a values of cementitious materials. The selection of the method used to estimate E_a should be based on the purpose of the maturity function used—whether it is for time of set, strength, or degree of hydration modeling. Physical properties besides hydration development such as porosity can affect the results of compressive strength, and presumably other mechanical properties such as elastic modulus.
- E_a values vary with the calculation techniques. The exponential method and ASTM C1074 hyperbolic function are in good agreement for total heat of hydration and the ASTM C1074 two steps method correlates with the E_a calculated using the ASTM C1074 hyperbolic function from mortar strength.
- Both initial and final setting times give similar response for E_a values, indicating that the initial and final setting are influenced equally by temperature.
- Both cement paste and mortar give similar E_a values for the same measurement and calculation method. This means that E_a calculated from cement pastes can be used for predicting physical property of concrete mixtures.
- Apart from mixtures containing water reducing admixtures, chemical shrinkage can be used to calculate E_a. The exponential-U method was found to give similar results to the exponential-E method for total heat of hydration, showing that the ultimate chemical shrinkage may be different at different curing temperatures.
- The higher apparent activation energy values calculated from total heat of hydration include the reaction after setting as opposed to those calculated from setting time measurements supports that the early hydration during the induction period is less sensitive to curing temperature than during the acceleration and deceleration period.

Acknowledgments

The writers acknowledge the support of Kansas State University throughout the research. Authors also acknowledge the contribution of John D. Foster of Boral Material Technologies, Inc. for supplying the fly ash materials.

References

[1] Glasstone, S., Laidler, K. J., and Eyring, H., *The Theory of Rate Processes: The Kinetics of Chemical Reactions, Viscosity, Diffusion, and Electrochemical Phenomena*, McGraw-Hill Book Company, New York, 1941.

[2] Taylor, H. F., *Cement Chemistry*, Academic Press, San Diego, CA, 1990, 475 pp.
[3] ASTM C1074, 2009, "Standard Practice for Estimating Concrete Strength by the Maturity Method," *Annual Book of ASTM Standards*, Vol. 04.02, ASTM International, West Conshohocken, PA, pp. 1–10.
[4] Hewlett, P., *Lea's Chemistry of Cement and Concrete*, Butterworth-Heinemann, New York, 2004.
[5] Kada-Benameur, H., Wirquin, E., and Duthoit, B., "Determination of Apparent Activation Energy of Concrete by Isothermal Calorimetry," *Cement Concrete Res.*, Vol. 30, No. 2, 2000, pp. 301–305.
[6] Wang, J., Yan, P., and Hongfa, Y., "Apparent Activation Energy of Concrete in Early Age Determined by Adiabatic Test," *J. Wuhan Univ. Technol.-Mater. Sci. Ed.*, Vol. 22, No. 3, 2007, pp. 537–541.
[7] Pinto, R. C. A. and Hover, K. C., "Application of Maturity Approach to Setting Time," *ACI Mater. J.*, Vol. 96, No. 6, 1999, pp. 686–691.
[8] Garcia, L., Castro-Fresno, D., and Polanco, J., "Maturity Approach Applied to Concrete by Means of Vicat Tests," *ACI Mater. J.*, Vol. 105, No. 5, 2008, pp. 445–450.
[9] Ma, W., Sample, D., Martin, R., and Brown, P. W., "Calorimetric Study of Cement Blends Containing Fly Ash, Silica Fume, and Slag at Elevated Temperatures," *Cement, Concrete, Aggregates*, Vol. 16, No. 2, 1994, pp. 93–99.
[10] Poole, J. L., Riding, K. A., Folliard, K. J., Juenger, M. C. G., and Schindler, A. K., "Methods for Calculating Activation Energy for Portland Cement," *ACI Mater. J.*, Vol. 104, No. 1, 2007, pp. 303–311.
[11] Tank, R. C. and Carino, N. J., "Rate Constant Functions for Strength Development of Concrete," *ACI Mater. J.*, Vol. 88, No. 1, 1991, pp. 74–83.
[12] ASTM C191, 2008, "Standard Test Methods for time of Setting of Hydraulic Cement by Vicat Needle," *Annual Book of ASTM Standards*, Vol. 04.01, ASTM International, West Conshohocken, PA, pp. 1–8.
[13] ASTM C403, 2008, "Standard Test Method for Time of Setting of Concrete Mixtures by Penetration Resistance," *Annual Book of ASTM Standards*, Vol. 04.02, ASTM International, West Conshohocken, PA, pp. 1–7.
[14] Schindler, A. K., "Effect of Temperature on Hydration of Cementitious Materials," *ACI Mater. J.*, Vol. 101, No. 1, 2004, pp. 72–81.
[15] Wirquin, E., Broda, M., and Duthoit, B., "Determination of the Apparent Activation Energy of One Concrete by Calorimetric and Mechanical Means: Influence of a Superplasticizer," *Cement Concrete Res.*, Vol. 32, No. 8, 2002, pp. 1207–1213.
[16] ASTM C618, 2008, "Standard Specification for Coal Fly Ash and Raw or Calcined Natural Pozzolan for Use in Concrete," *Annual Book of ASTM Standards*, Vol. 04.02, ASTM International, West Conshohocken, PA, pp. 1–3.
[17] ASTM C989, 2010, "Standard Specification for Slag Cement for Use in Concrete and Mortars," *Annual Book of ASTM Standards*, Vol. 04.02, ASTM International, West Conshohocken, PA, pp. 1–6.
[18] Rietveld, H. M., "A Profile Refinement Method for Nuclear and Magnetic Structure," *J. Appl. Crystallogr.*, Vol. 2, 1969, pp. 65–71.
[19] ASTM C150, 2011, "Standard Specification for Portland Cement," *Annual Book of ASTM Standards*, Vol. 04.01, ASTM International, West Conshohocken, PA, pp. 1–9.

[20] ASTM C33, 2003, "Standard Specification for Concrete Aggregates," *Annual Book of ASTM Standards*, Vol. 04.02, ASTM International, West Conshohocken, PA, pp. 1–11.
[21] ASTM C305, 1999, "Standard Practice for Mechanical Mixing of Hydraulic Cement Pastes and Mortars of Plastic Consistency," *Annual Book of ASTM Standards*, Vol. 04.01, ASTM International, West Conshohocken, PA, pp. 1–3.
[22] ASTM C109, 2011, "Standard Test Method for Compressive Strength of Hydraulic Cement Mortars (Using 2-in. or [50-mm] Cube Specimens)," *Annual Book of ASTM Standards*, Vol. 04.01, ASTM International, West Conshohocken, PA, pp. 1–10.
[23] Freiesleben-Hansen, P. and Pedersen, E. J., "Maturity Computer for Controlling Curing and Hardening of Concrete," *Nordisk Betong*, Vol. 1, No. 19, 1977, pp. 21–25.
[24] García, A., Castro-Fresno, D., and Polanco, J. A., "Evolution of Penetration Resistance in Fresh Concrete," *Cement Concrete Res.*, Vol. 38, No. 5, 2008, pp. 649–659.
[25] Bentz, D. P., Peltz, A. M., and Winpigler, J., "Early-Age Properties of Cement-Based Materials. II: Influence of Water-to-Cement Ratio," *J. Mater. Civil Eng.*, Vol. 21, No. 9, 2009, pp. 512–517.
[26] Broda, M., Wirquin, E., and Duthoit, B., "Conception of an Isothermal Calorimeter for Concrete-Determination of the Apparent Activation Energy," *Mater. Struct.*, Vol. 35, No. 251, 2002, pp. 389–394.
[27] Geiker, M., *Studies of Portland Cement Hydration: Measurements of Chemical Shrinkage and a Systematic Evaluation of Hydration Curves by Means of the Dispersion Model*, Technical University of Denmark, Copenhagen, Denmark, 1983.
[28] ASTM C1608, 2005, "Standard Test Method for Chemical Shrinkage of Hydraulic Cement Paste," *Annual Book of ASTM Standards*, Vol. 04.01, ASTM International, West Conshohocken, PA, pp. 1–4.
[29] Sant, G., Lura, P., and Weiss, J., "Measurement of Volume Change in Cementitious Materials at Early Ages: Review of Testing Protocols and Interpretation of Results," *Transp. Res. Rec.*, No. 2006, 1979, pp. 21–29.
[30] Knudsen, T. and Geiker, M., "Obtaining Hydration Data by Measurement of Chemical Shrinkage With an Archimeter," *Cement Concrete Res.*, Vol. 15, 1985, pp. 381–382.
[31] Siddiqui, M. S., *Effect of Temperature and Curing on the Early Hydration of Cementitious Materials*, Kansas State University, Manhattan, KS, 2010.
[32] Bentz, D. P., "Modeling the Influence of Limestone Filler on Cement Hydration Using CEMHYD3D," *Cement Concrete Composites*, Vol. 28, 2006, pp. 124–129.
[33] Zhang, J., Weissinger, E. A., Peethamparan, S., and Scherer, G. W., "Early Hydration and Setting of Oil Well Cement," *Cement Concrete Res.*, Vol. 40, 2010, pp. 1023–1033.
[34] Zhang, X., *Quantitative Microstructural Characterization of Concrete Cured Under Realistic Temperature Conditions*, Swiss Federal Institute of Technology at Lausanne, Lausanne, Switzerland, 2007, 230 pp.